Global Ocean Tripole and Climate Variability

Peter C. Chu
Naval Postgraduate School

EAPS, MIT June 2, 2010

Outline

- (1) Recent Development in Short-term Climate Variability
- (2) Data Analysis: (T, S) Profiles → Synoptic Gridded Data with Monthly Increment
- (3) Synoptic Upper Ocean (0-300 m) Heat Content
- (4) Global Tripole → Canonical El Nino, El Nino Modoki, Indian Ocean Dipole, …

(1) Recent Development in Climate Variability

Indian Ocean Dipole
El Nino Modoki

Indian Ocean Dipole (Saji et al. 1999)

Positive Dipole Mode

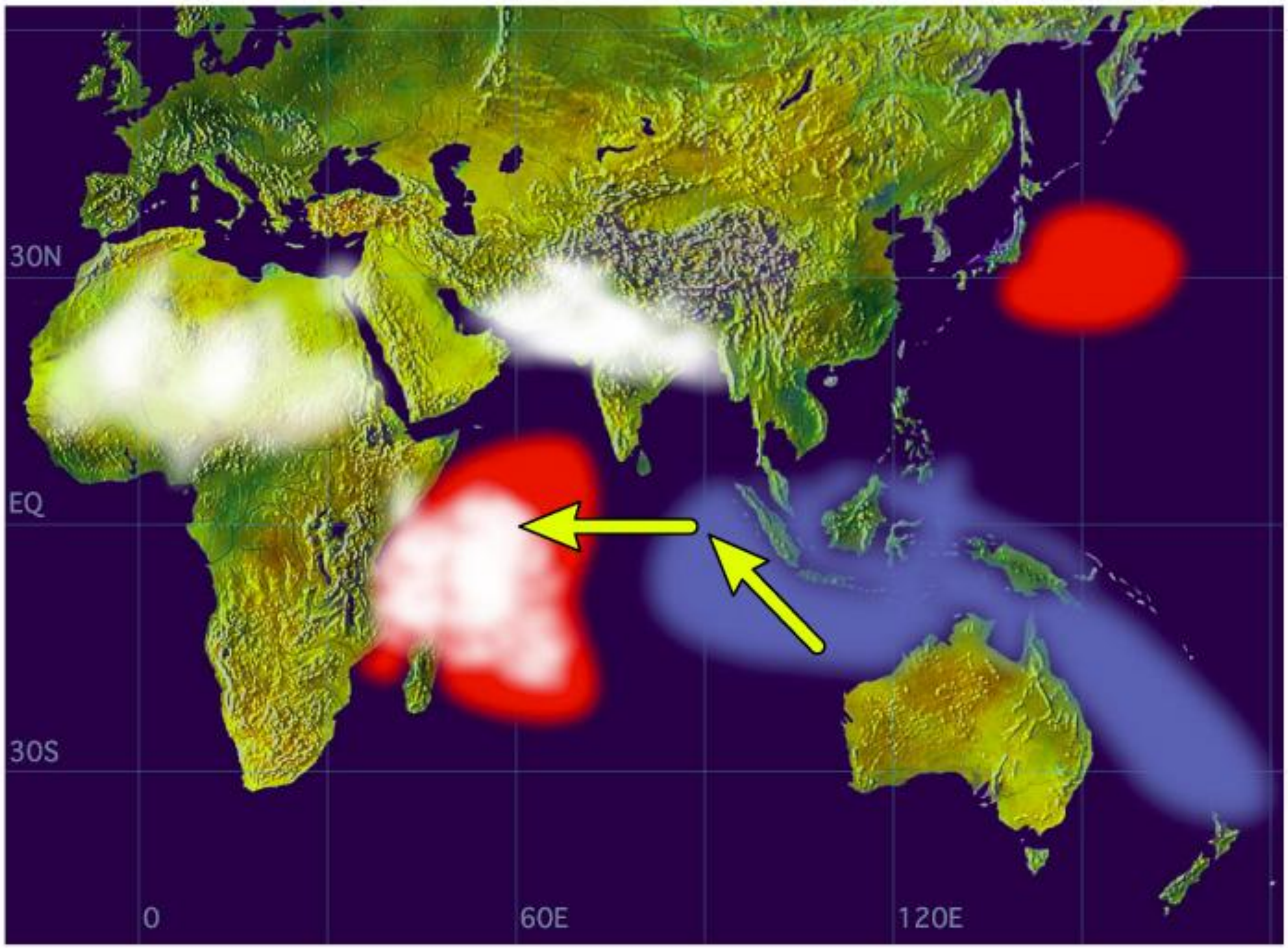

Indian Ocean Dipole (Saji et al. 1999)

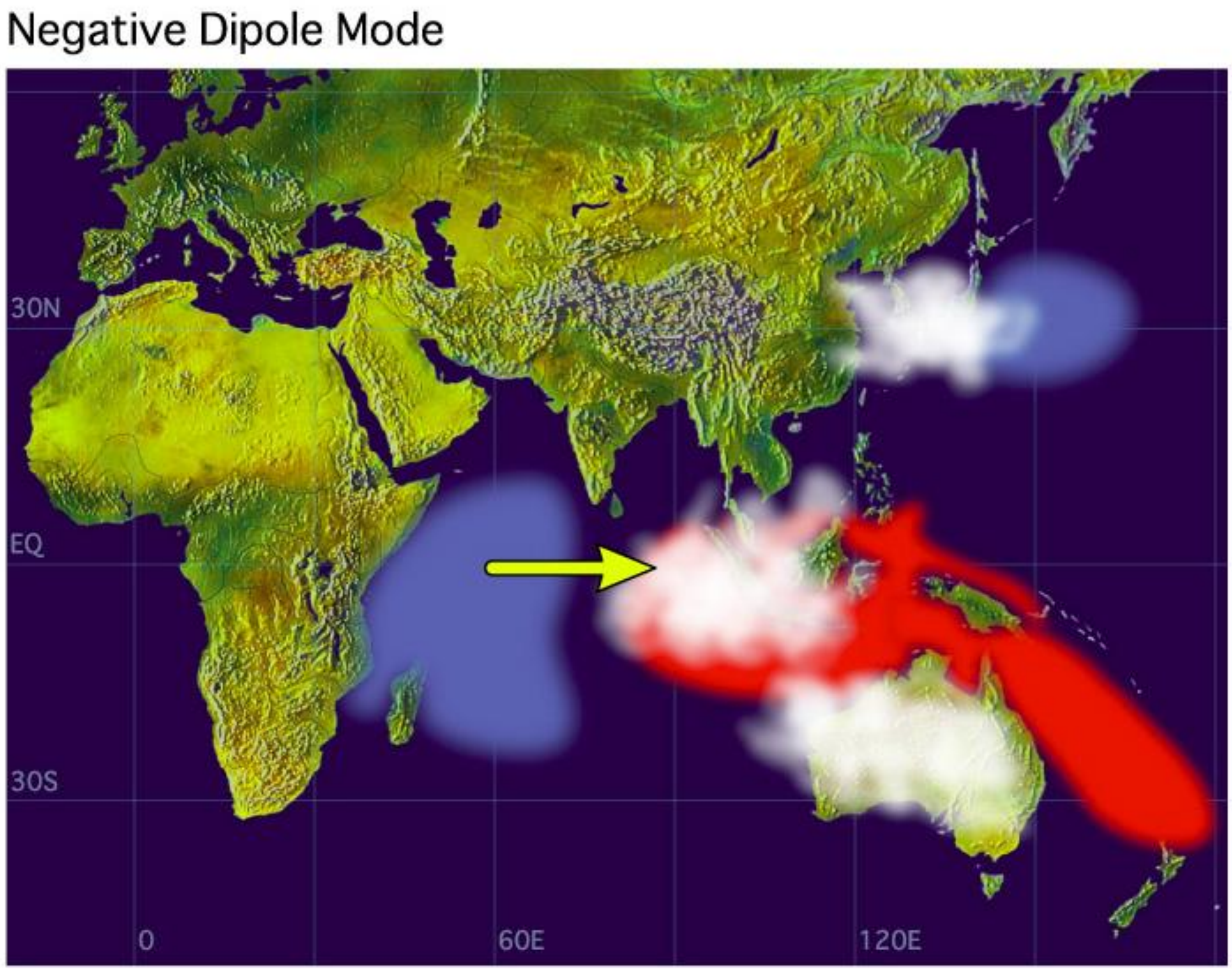

El Nino and El Nino Modoki

(Weng et al. 2007, Ashok et al. 2007)

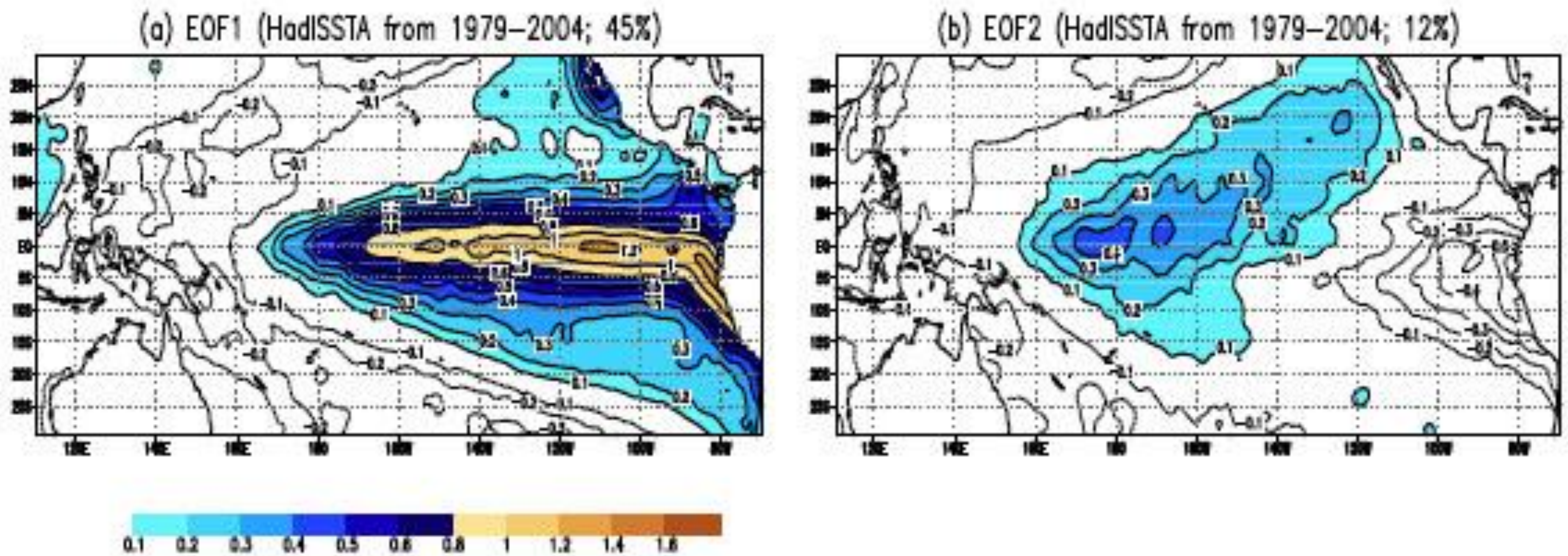

(Images courtesy Karumuri Ashok, APEC Climate Center)

(2). Data Analysis

Global Temperature and Salinity Profile Program (GTSPP)

GTSPP

GTSPP = Global Temperature Salinity Profile Program

- GTSPP is a joint WMO-IOC program designed to provide improved access to the highest resolution, highest quality data as quickly as possible.
- GTSPP began as an official IODE pilot project in 1989.
- It went into operation in November 1990.

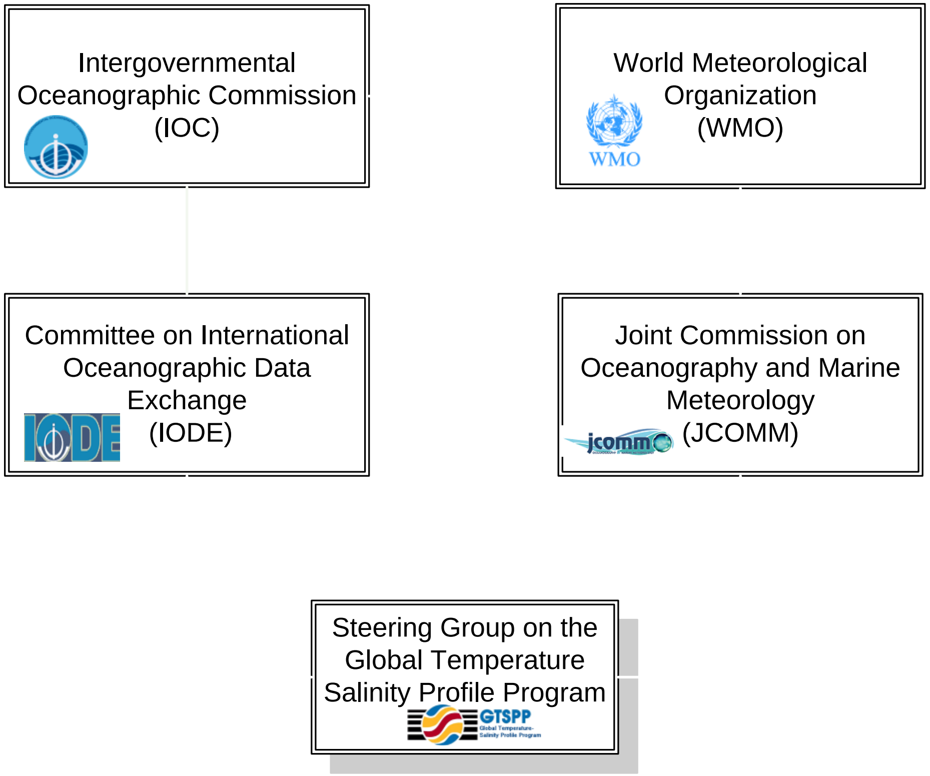

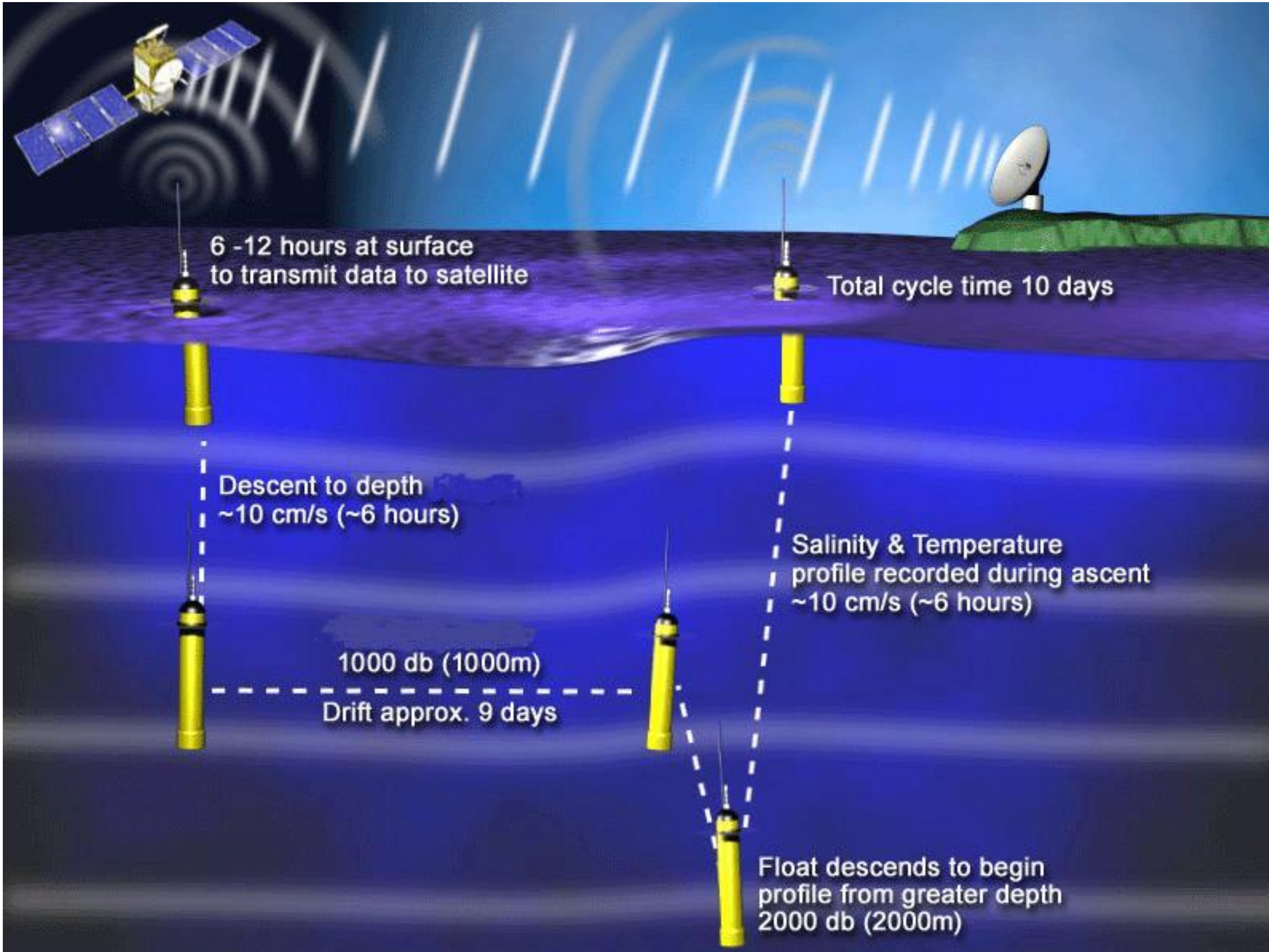
6 -12 hours at surface
to transmit data to satellite
Total cycle time 10 days
Descent to depth
~10 cm/s (~6 hours)
Salinity & Temperature
profile recorded during ascent
~10 cm/s (~6 hours)
1000 db (1000m)
Drift approx. 9 days
Float descends to begin
profile from greater depth
2000 db (2000m)

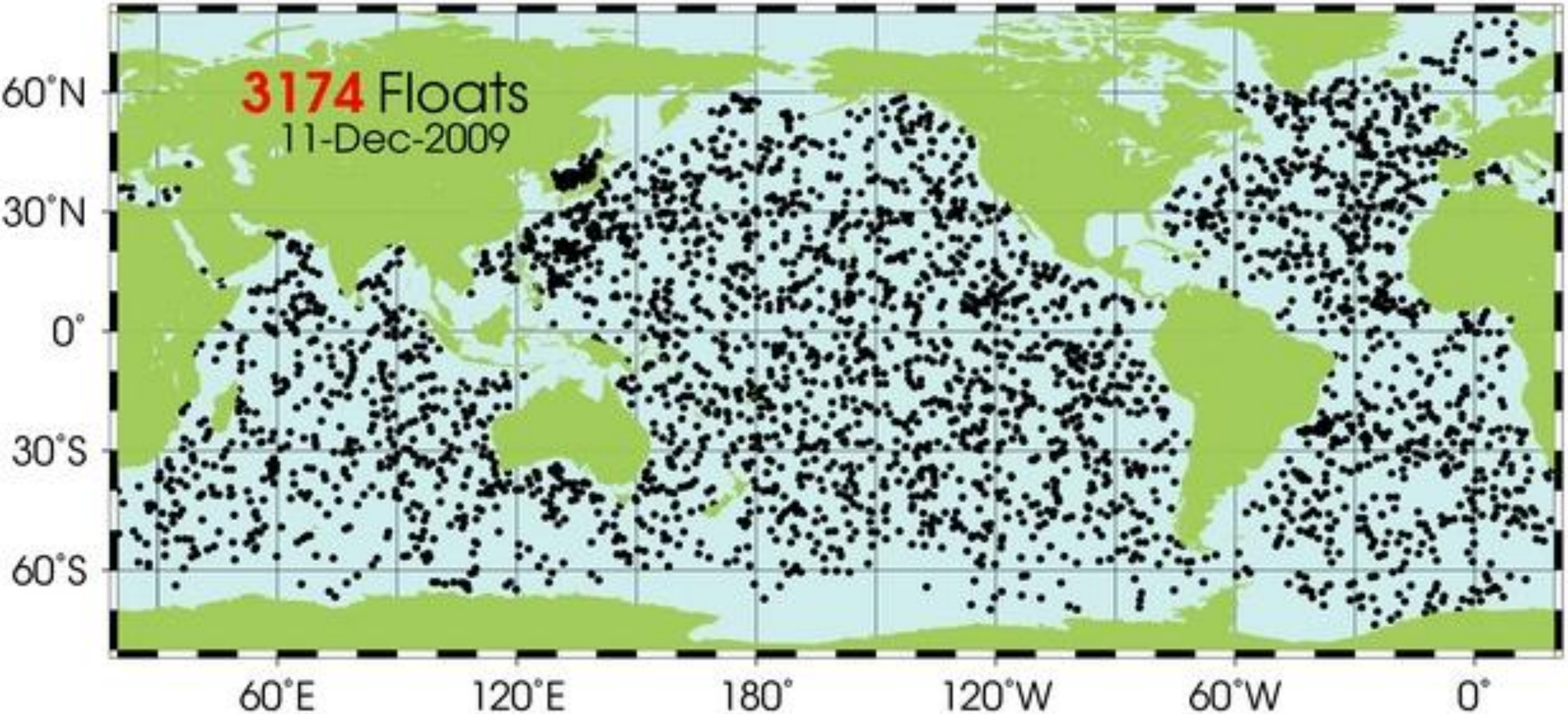
3174 Floats
11-Dec-2009
60°N
30°N
0°
30°S
60°S
60°E
120°E
180°
120°W
60°W
0°

Example → GTSPP Data

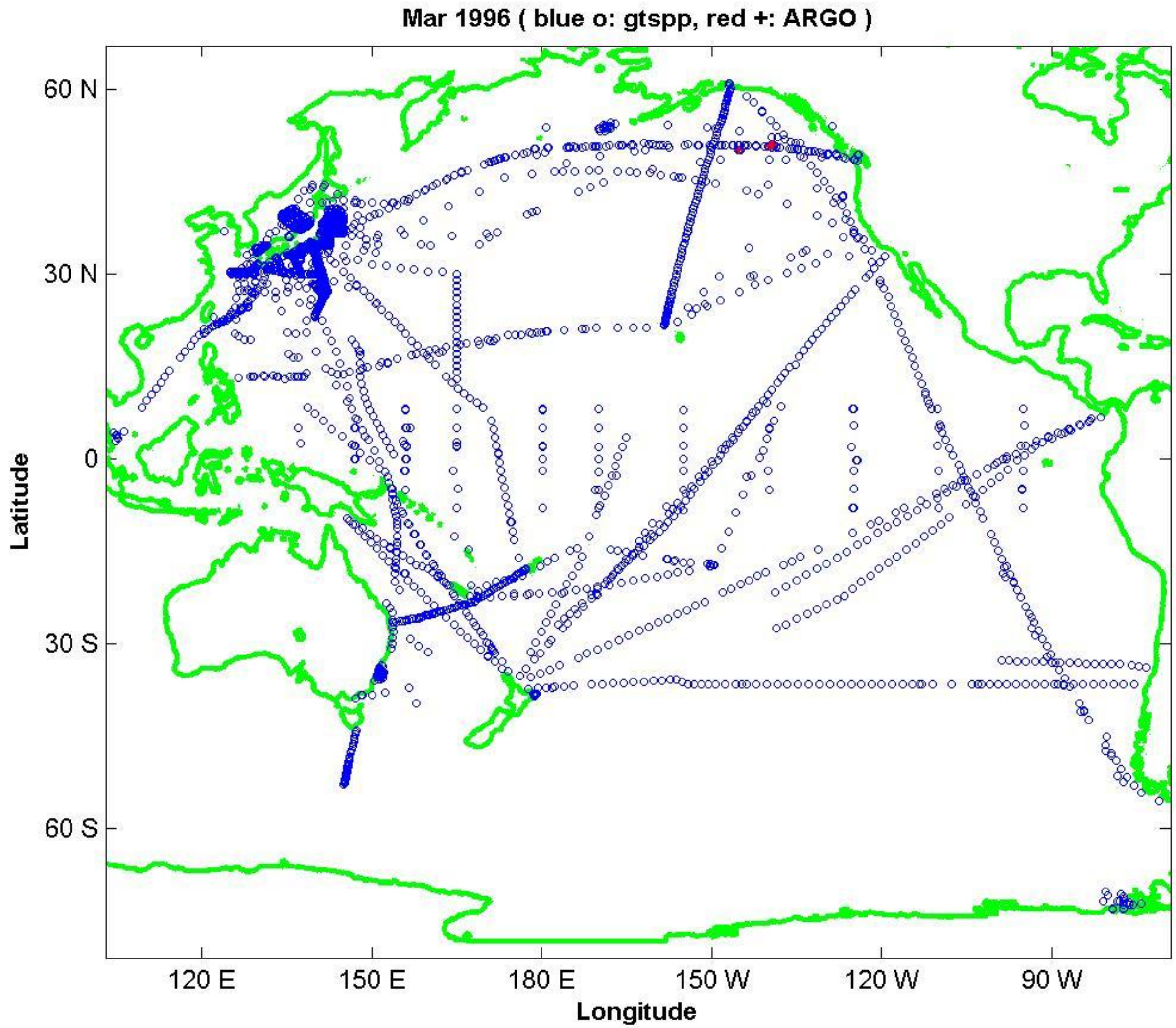

Ocean Data Analysis

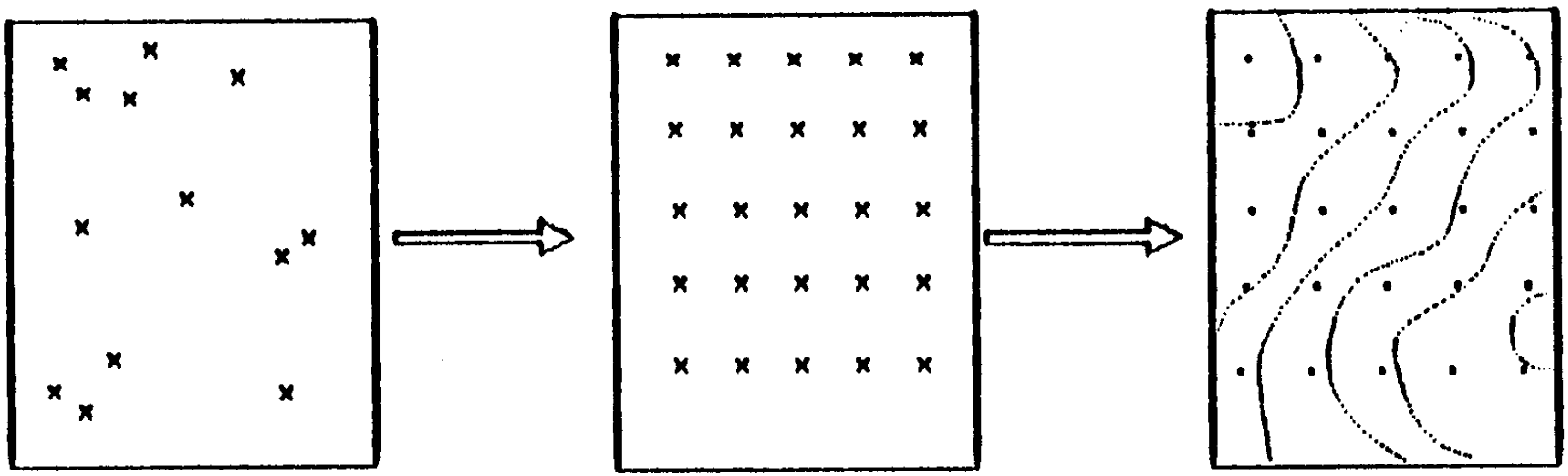

Classical Method → Fourier Series Expansion

Joseph Fourier 1768-1830

Fourier was obsessed with the physics of heat and developed the Fourier series and transform to model heat-flow problems.

Fourier Series Expansion

For a rectangular region (L_x, L_y), the basis functions are sinusoidal functions.

$$f(x,y) = \sum_i \sum_j a_{ij} \sin\frac{i\pi x}{L_x} \sin\frac{j\pi y}{L_y}$$

$$+ \sum_i \sum_j b_{ij} \cos\frac{i\pi x}{L_x} \cos\frac{j\pi y}{L_y}$$

For the Dirichret boundary condition : $f = 0$ at the boundaries

$$f(x,y) = \sum_i \sum_j a_{ij} \sin\frac{i\pi x}{L_x} \sin\frac{j\pi y}{L_y}$$

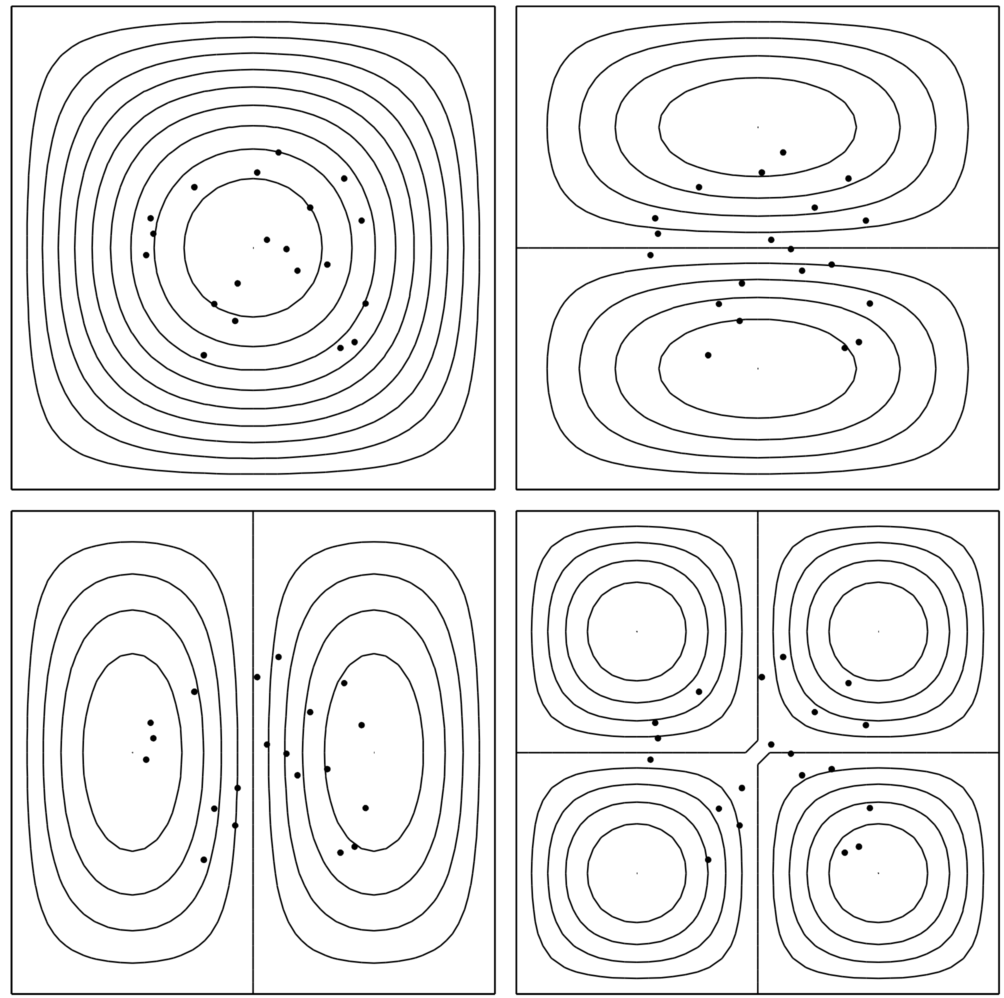

The dots represent the Observations.

Linear Algebraic Equations for the Coefficients a_{ij}

$$f(x_1^{ob}, y_1^{ob}) = \sum_i \sum_j a_{ij} \sin\frac{i\pi x_1^{ob}}{L_x} \sin\frac{j\pi y_1^{ob}}{L_y}$$

$$f(x_2^{ob}, y_2^{ob}) = \sum_i \sum_j a_{ij} \sin\frac{i\pi x_2^{ob}}{L_x} \sin\frac{j\pi y_2^{ob}}{L_y}$$

……

$$f(x_M^{ob}, y_M^{ob}) = \sum_i \sum_j a_{ij} \sin\frac{i\pi x_M^{ob}}{L_x} \sin\frac{j\pi y_M^{ob}}{L_y}$$

Determination of Spectral Coefficients (Ill-Posed Algebraic Equation)

$$\mathbf{A}\hat{\mathbf{a}} = \mathbf{Q}\mathbf{Y},$$

Known a_{ij} → Analyzed Field

$$f(x,y) = \sum_i \sum_j a_{ij} \sin\frac{i\pi x}{L_x} \sin\frac{j\pi y}{L_y}$$

For the Neumann boundary condition $n \bullet \nabla f = 0$ at the boundaries

$$f(x, y) = \sum_i \sum_j b_{ij} \cos\frac{i\pi x}{L_x} \cos\frac{j\pi y}{L_y}$$

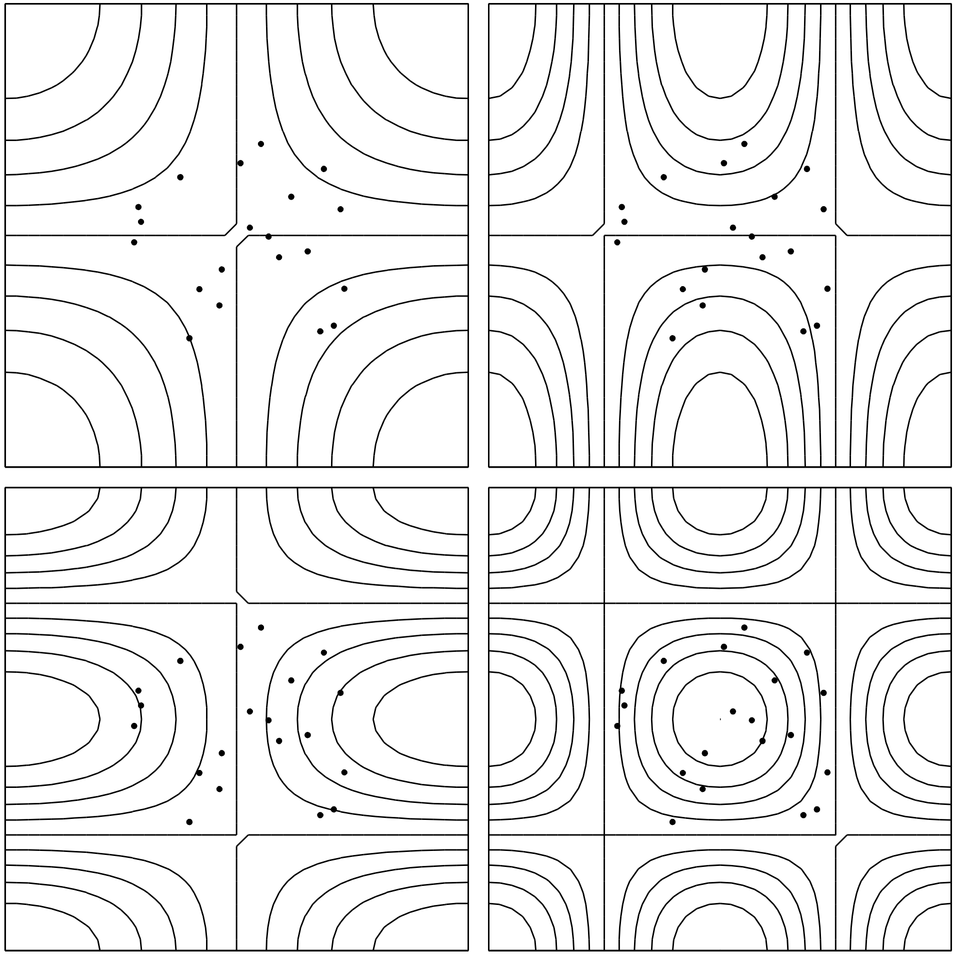

The dots represent the Observations.

Linear Algebraic Equations for the Coefficients a_{ij}

$$f(x_1^{ob}, y_1^{ob}) = \sum_i \sum_j b_{ij} \cos\frac{i\pi x_1^{ob}}{L_x} \cos\frac{j\pi y_1^{ob}}{L_y}$$

$$f(x_2^{ob}, y_2^{ob}) = \sum_i \sum_j b_{ij} \cos\frac{i\pi x_2^{ob}}{L_x} \cos\frac{j\pi y_2^{ob}}{L_y}$$

……

$$f(x_M^{ob}, y_M^{ob}) = \sum_i \sum_j b_{ij} \cos\frac{i\pi x_M^{ob}}{L_x} \cos\frac{j\pi y_M^{ob}}{L_y}$$

Known b_{ij} → Analyzed Field

$$f(x,y) = \sum_i \sum_j b_{ij} \cos\frac{i\pi x}{L_x} \cos\frac{j\pi y}{L_y}$$

For General Ocean Basin → Generalized Fourier Series Expansion

Spectral Representation
Fourier Series Expansion

$$c(\mathbf{x}, z_k, t) = A_0(z_k, t) + \sum_{m=1}^{M} A_m(z_k, t)\ \Psi_m(\mathbf{x}, z_k),$$

Ψ_m → Basis functions (not sinusoidal)

c → any ocean variable

Determination of Basis Functions

- (1) Eigen Functions of the Laplace Operator (Data and Model Independent)

- (2) Empirical Orthogonal Functions (Data or Model Dependent)

Eigen Functions of Laplace Operator → Basis Functions (Closed Basin)

$$\Delta\Psi_k = -\lambda_k\Psi_k, \quad \Psi_k|_\Gamma = 0, \qquad k = 1, ..., \infty$$

$$\Delta\Phi_m = -\mu_m\Phi_m, \quad \frac{\partial\Phi_m}{\partial n}|_\Gamma = 0, \qquad m = 1, ..., \infty.$$

Ψ_k → Streamfunction

Φ_m → T, S, Velocity Potential

Basis Functions
(Open Boundaries)

$$\triangle \Psi_k = -\lambda_k \Psi_k,$$

$$\triangle \Phi_m = -\mu_m \Phi_m,$$

$$\Psi_k|_\Gamma = 0, \quad \frac{\partial \Phi_m}{\partial n}|_\Gamma = 0,$$

$$\left[\frac{\partial \Psi_k}{\partial n} + \kappa(\tau)\Psi_k\right]|_{\Gamma_1'} = 0, \quad \Phi_m|_{\Gamma_1'} = 0,$$

Boundary Conditions

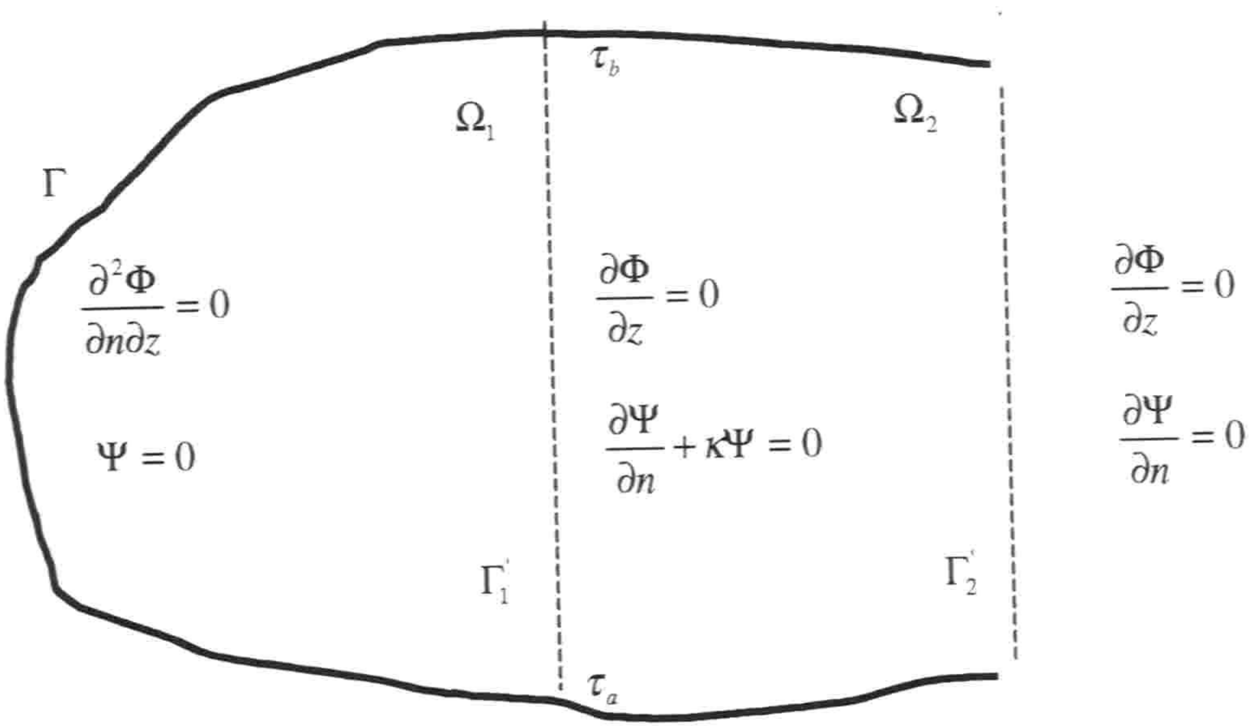

Spectral Decomposition

$$u_{KM} = \sum_{k=1}^{K} a_k(z, t^\circ) \frac{\partial \Psi_k(x, y, z, \kappa^\circ)}{\partial y} + \sum_{m=1}^{M} b_m(z, t^\circ) \frac{\partial \Phi_m(x, y, z)}{\partial x},$$

$$v_{KM} = -\sum_{k=1}^{K} a_k(z, t^\circ) \frac{\partial \Psi_k(x, y, z, \kappa^\circ)}{\partial x} + \sum_{m=1}^{M} b_m(z, t^\circ) \frac{\partial \Phi_m(x, y, z)}{\partial y}$$

$$T(\mathbf{x}, t) = T_0(\mathbf{x}) + \sum_{m=1}^{M} c_m(t) \Phi_m(\mathbf{x})$$

$$S(\mathbf{x}, t) = S_0(\mathbf{x}) + \sum_{m=1}^{M} d_m(t) \Phi_m(\mathbf{x})$$

Benefits of Using OSD

- (1) Don’t need first guess field
- (2) Don’t need autocorrelation functions
- (3) Don’t require high signal-to-noise ratio
- (4) Basis functions are pre-determined before the data analysis. They are independent on the data.

Optimal Mode Truncation

$$J(a_{1,\dots,}a_K, b_{1,\dots,}b_M, \kappa, P) = \frac{1}{2}\left(\left\|u_p^{obs} - u_{KM}\right\|_P^2 + \left\|v_p^{obs} - v_{KM}\right\|_P^2\right) \rightarrow \min,$$

Vapnik (1983) Cost Function

$$J_{emp} = J(a_{1,\ldots,}a_{K,}b_{1,\ldots,}b_{M}, \kappa, P).$$

$$\text{Prob}\left\{\sup_{K,M,S} |\langle J(K,M,S)\rangle - J_{emp}(K,M,S)| \geq \mu\right\} \leq g(P,\mu)$$

$$\lim_{P\to\infty} g(P,\mu) = 0$$

Optimal Truncation

- Gulf of Mexico, Monterey Bay, Louisiana-Texas Shelf, North Atlantic

- $K_{opt} = 40$, $M_{opt} = 30$

Determination of Spectral Coefficients (Ill-Posed Algebraic Equation)

$$\mathbf{A}\hat{\mathbf{a}} = \mathbf{Q}\mathbf{Y},$$

This is caused by the features of the matrix **A**.

Rotation Method (Chu et al., 2004)

Well-Posed → $$\mathbf{SA}\hat{\mathbf{a}} = \mathbf{SQY},$$

The matrix S is determined by

$$J_1 = \|\mathbf{A}\|^2 - \frac{\|\mathbf{SQY}\|^2}{\|\mathbf{a}\|^2} \rightarrow \max,$$

Errors

$$\bar{T}(\mathbf{x}) = \overbrace{T_0 + \sum_{l=1}^{48} D_l \Phi_l(\mathbf{x})}^{\hat{T}} + T'(\mathbf{x})$$

$$\bar{\mathbf{u}}(\mathbf{x},t) = \overbrace{C\Psi_0 + \sum_{n=1}^{24} A_n \nabla \times \mathbf{k}\Psi_n(\mathbf{x})}^{\hat{\mathbf{u}}} + \tilde{\mathbf{u}}(\mathbf{x}) + \mathbf{u}'(\mathbf{x})$$

T’ , **u**’ → errors

Noise-to-Signal Ratio → Error Estimation

$$\eta\left(\boldsymbol{\alpha}, \boldsymbol{\beta}\right) = \frac{\left\|\boldsymbol{\alpha}\right\|_{(P)}}{\left\|\boldsymbol{\beta}\right\|_{(P)}}$$

$$\eta(T', T - T') \sim 0.1$$

(3) Upper Ocean Heat Content

Upper Ocean (0-300 m) Heat Content

$$HC = \int_{-h}^{0} \rho c T dz$$

$HC = HC_{\text{mean}} + HC_{\text{seasonal}} + HC_{\text{anomaly}}$

EOF Analysis → HC_{anomaly}

→ Global Ocean Dipole Modes

Trend of Upper Ocean (0-700 m) Heat Content

0.4 X 10^{22} J/yr
(1958-2008)
(Levitus et al.,GRL, 2009)
Without Argo data

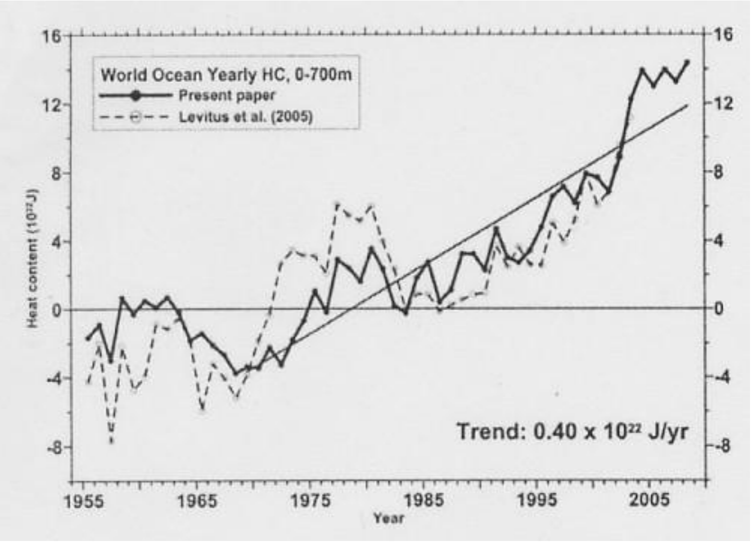

1.3 X 10^{22} J/yr
(1990-2008)

With Argo data

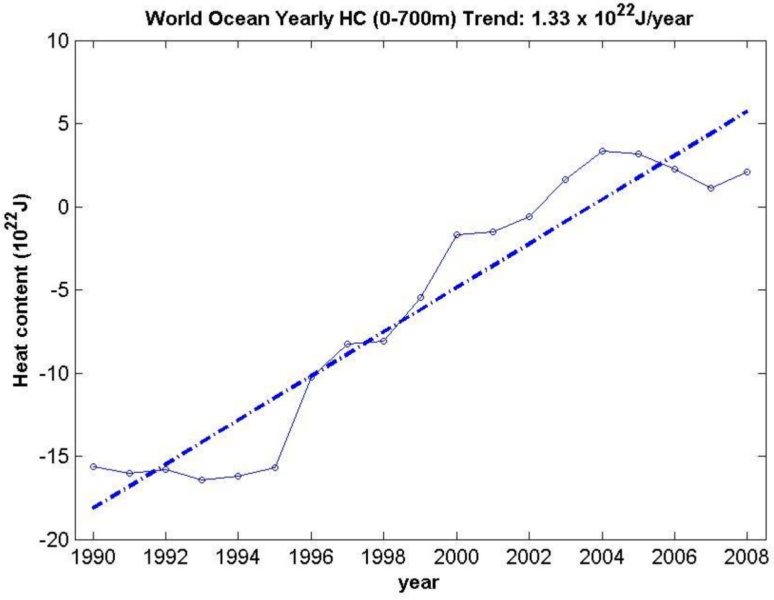

Upper Ocean (0-300 m) Mean Heat Content (J/m^2) (1990-2009)

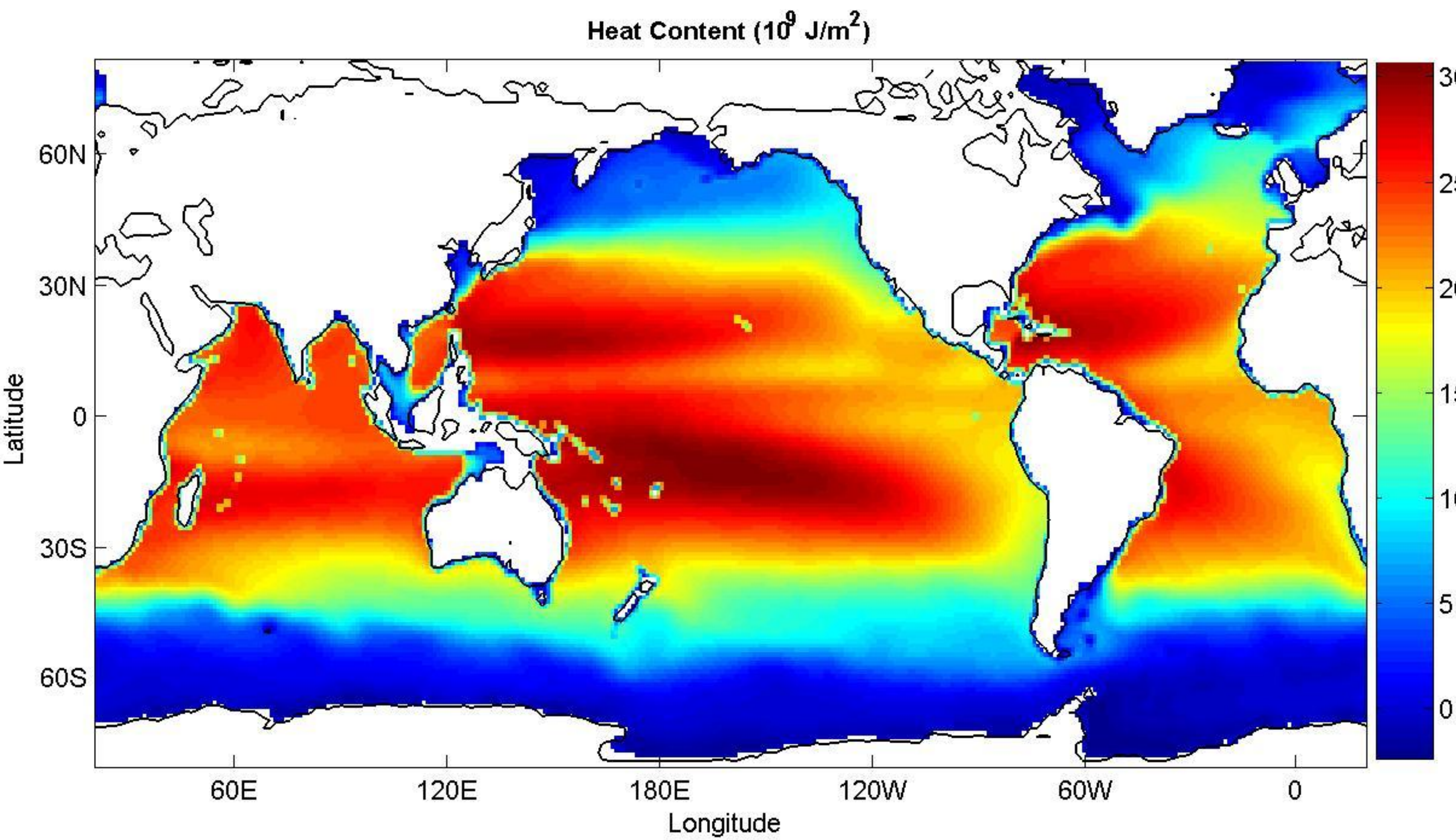

Seasonal Variability of Upper Ocean (0-300 m) Heat Content (J/m^2) (1990-2009)

January

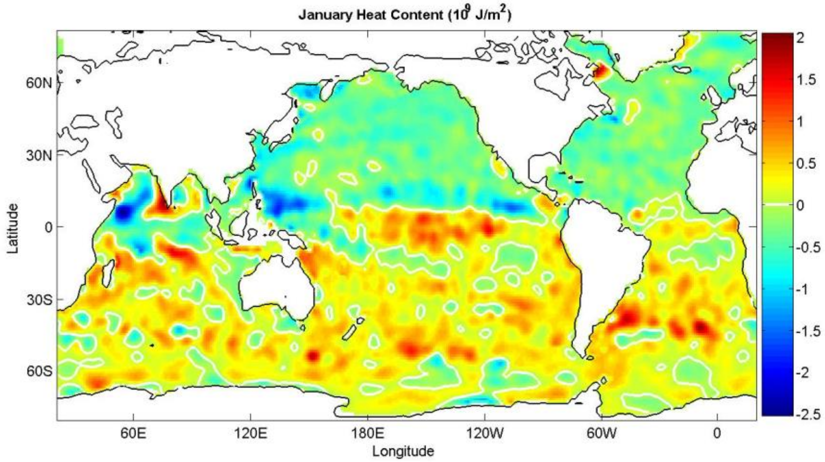

April

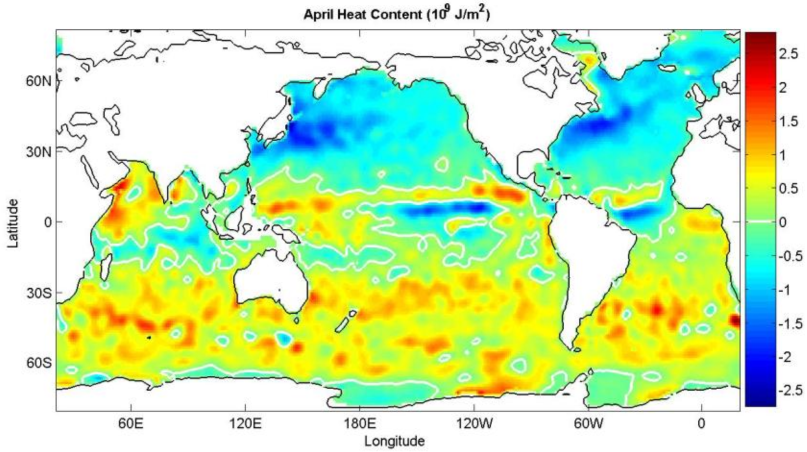

July

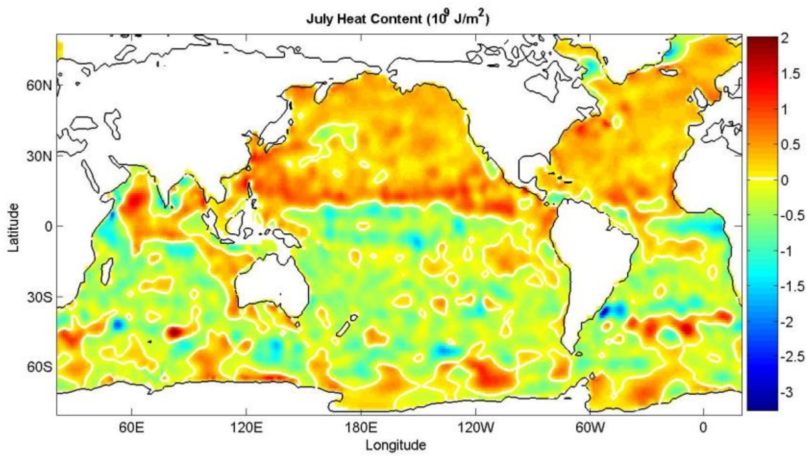

October

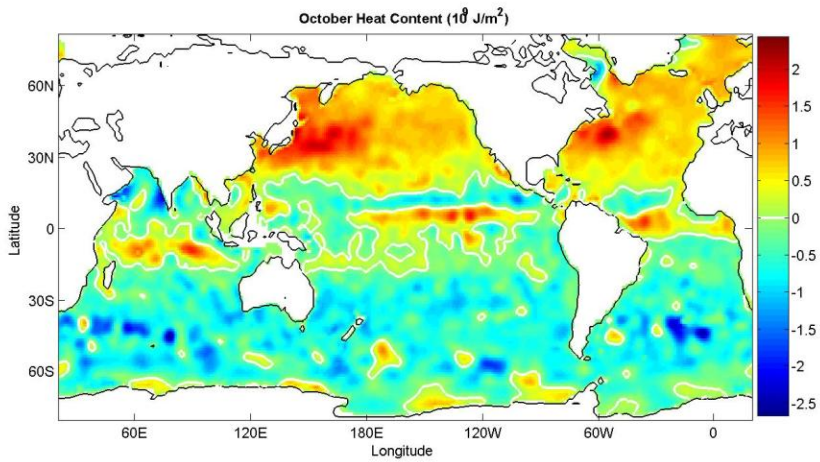

EOF Analysis →

Heat Content Anomaly Relative to Seasonal Variation

EOF-1 (in 10^8 J/m^2)

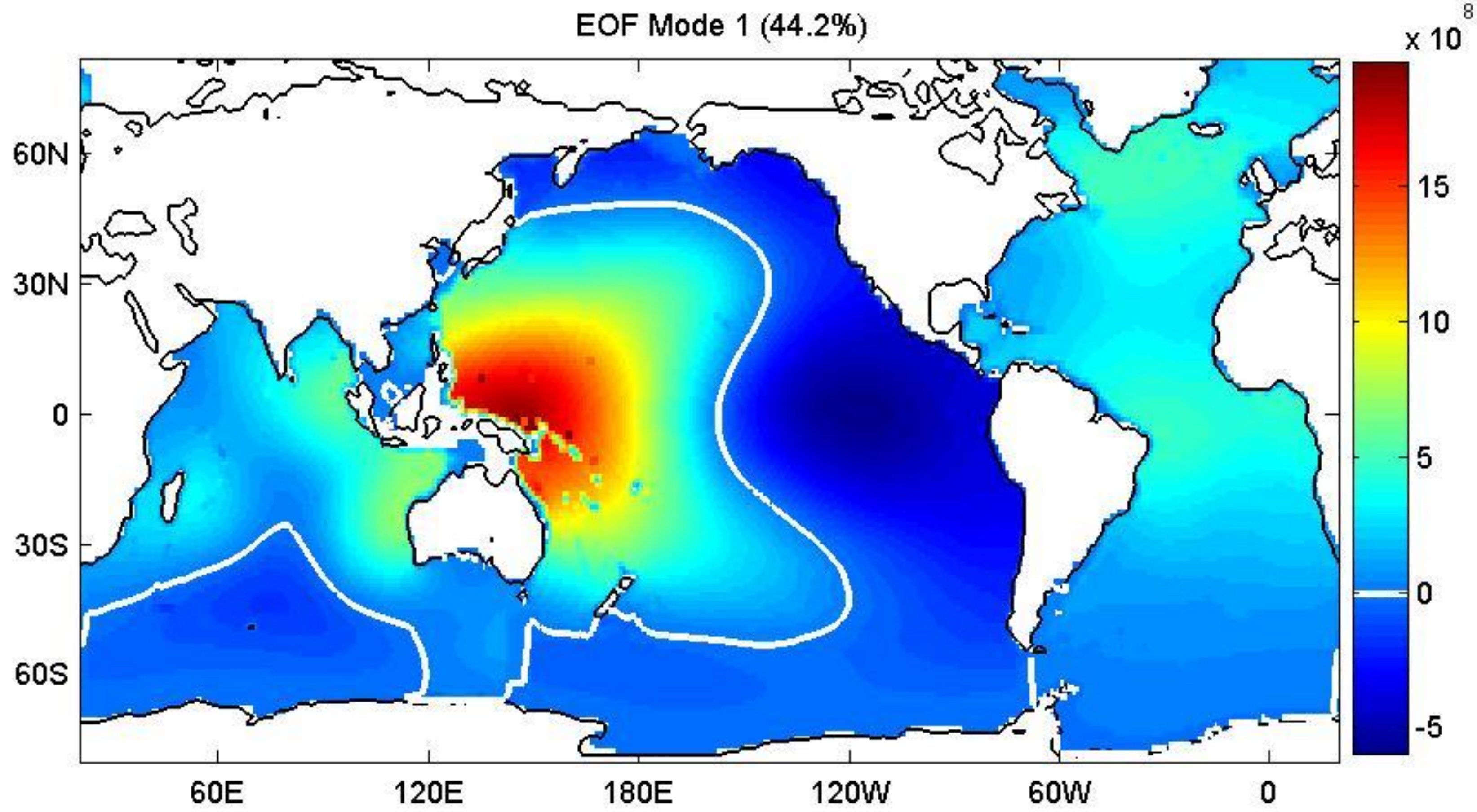

EOF-1 (in 10^8 J/m^2)

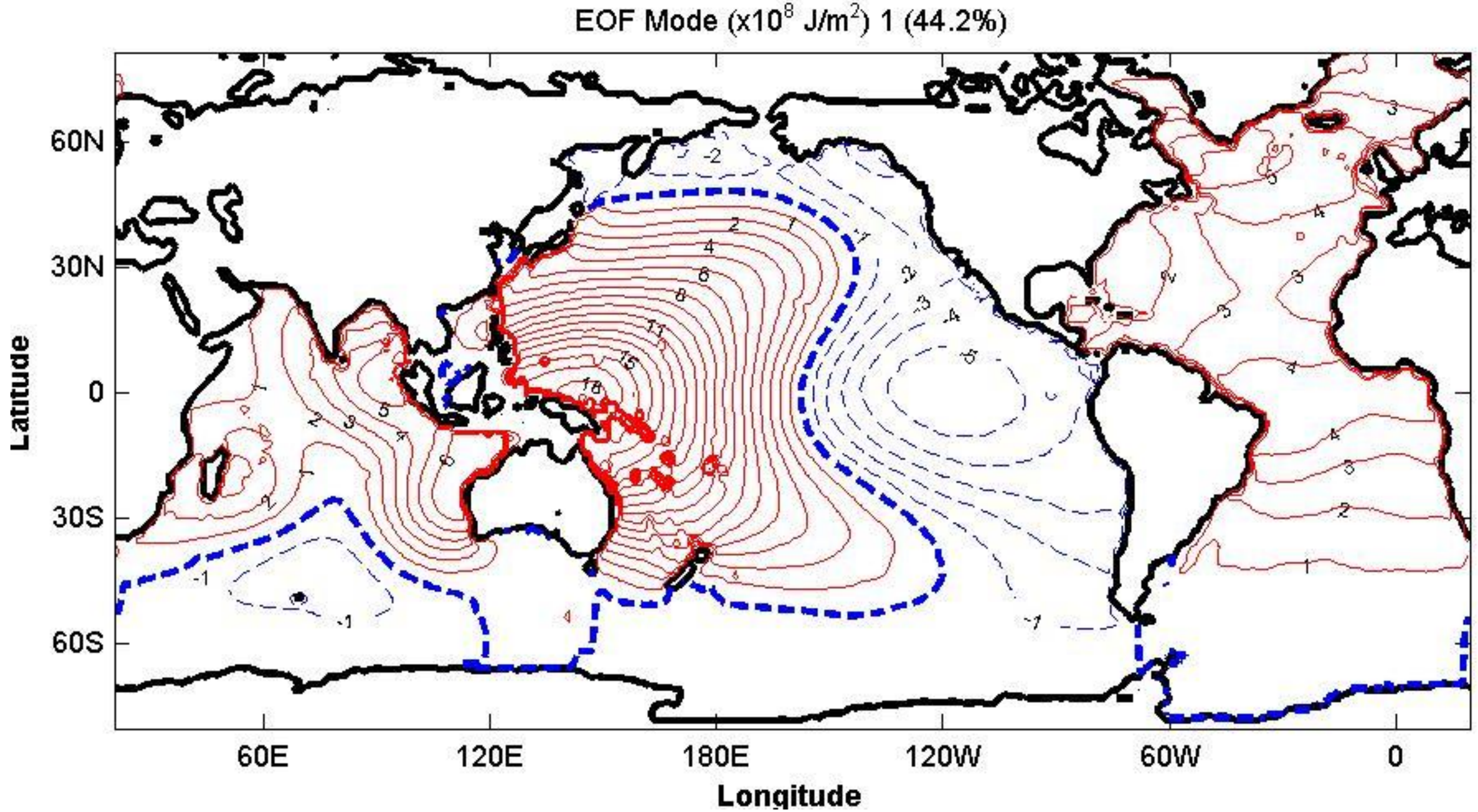

PC_1

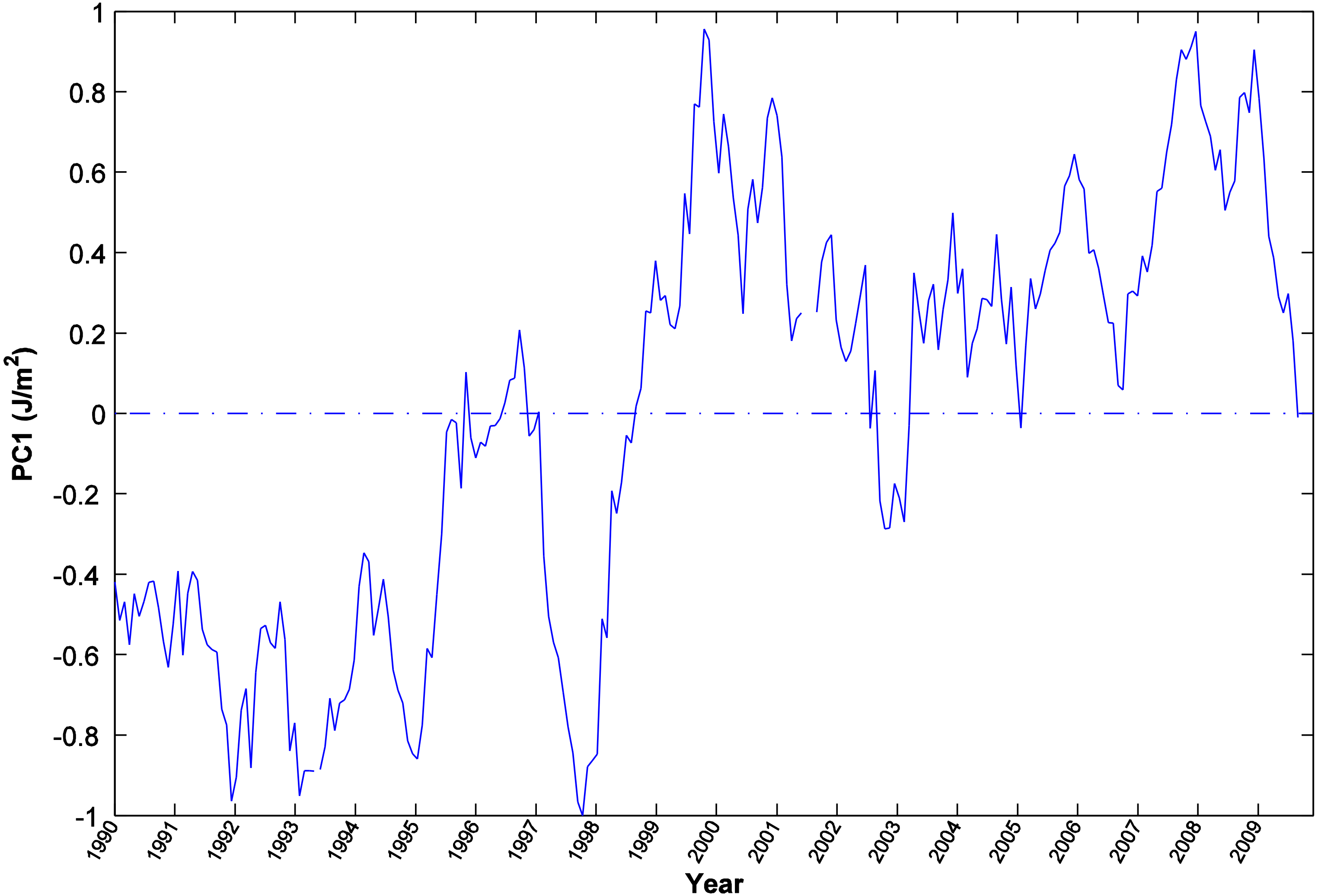

1
0.8
0.6
0.4
0.2
0
-0.2
-0.4
-0.6
-0.8
-1
PC1 (J/m2)
1990
1991
1992
1993
1994
1995
1996
1997
1998
1999
2000
2001
2002
2003
2004
2005
2006
2007
2008
2009
Year

Lag Correlation between PC_1 and SOI

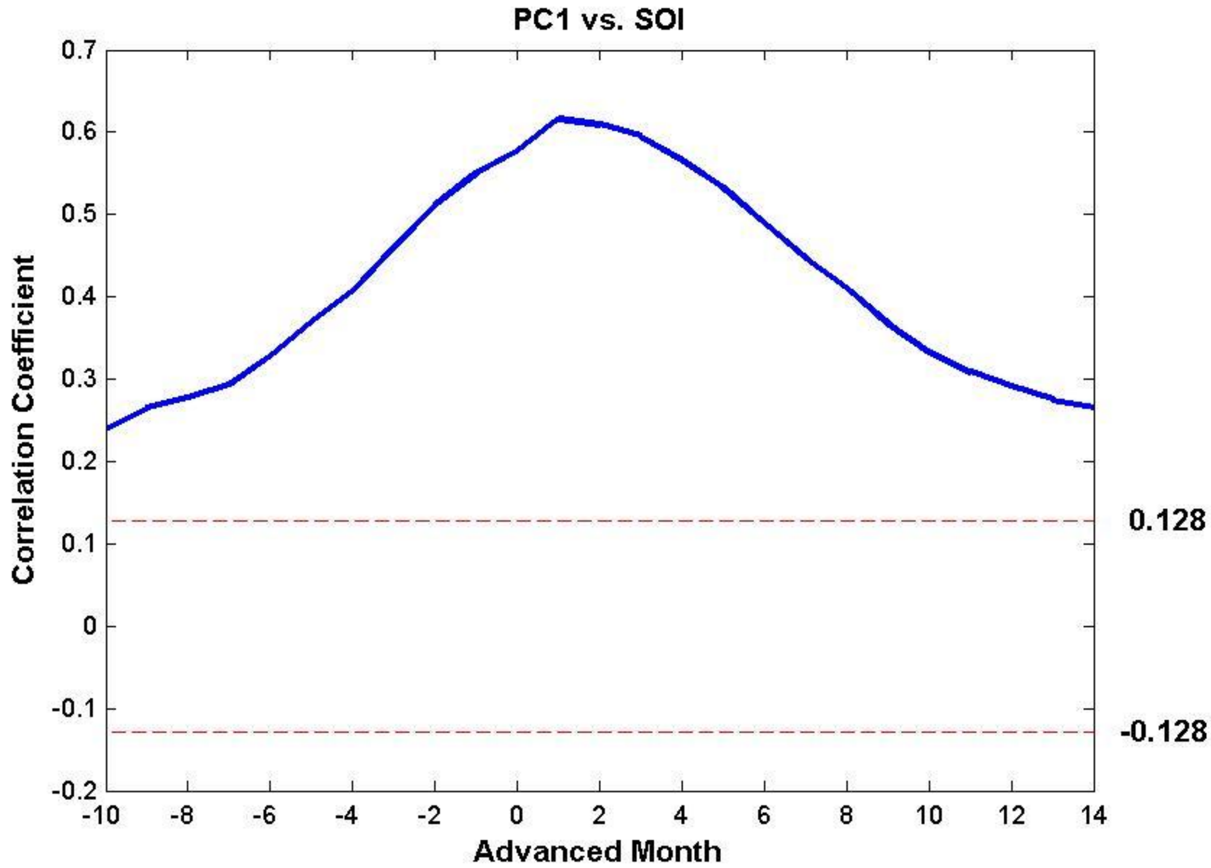

Positive Month → PC_1 advancing SOI

EOF-2 (in 10^8 J/m^2)

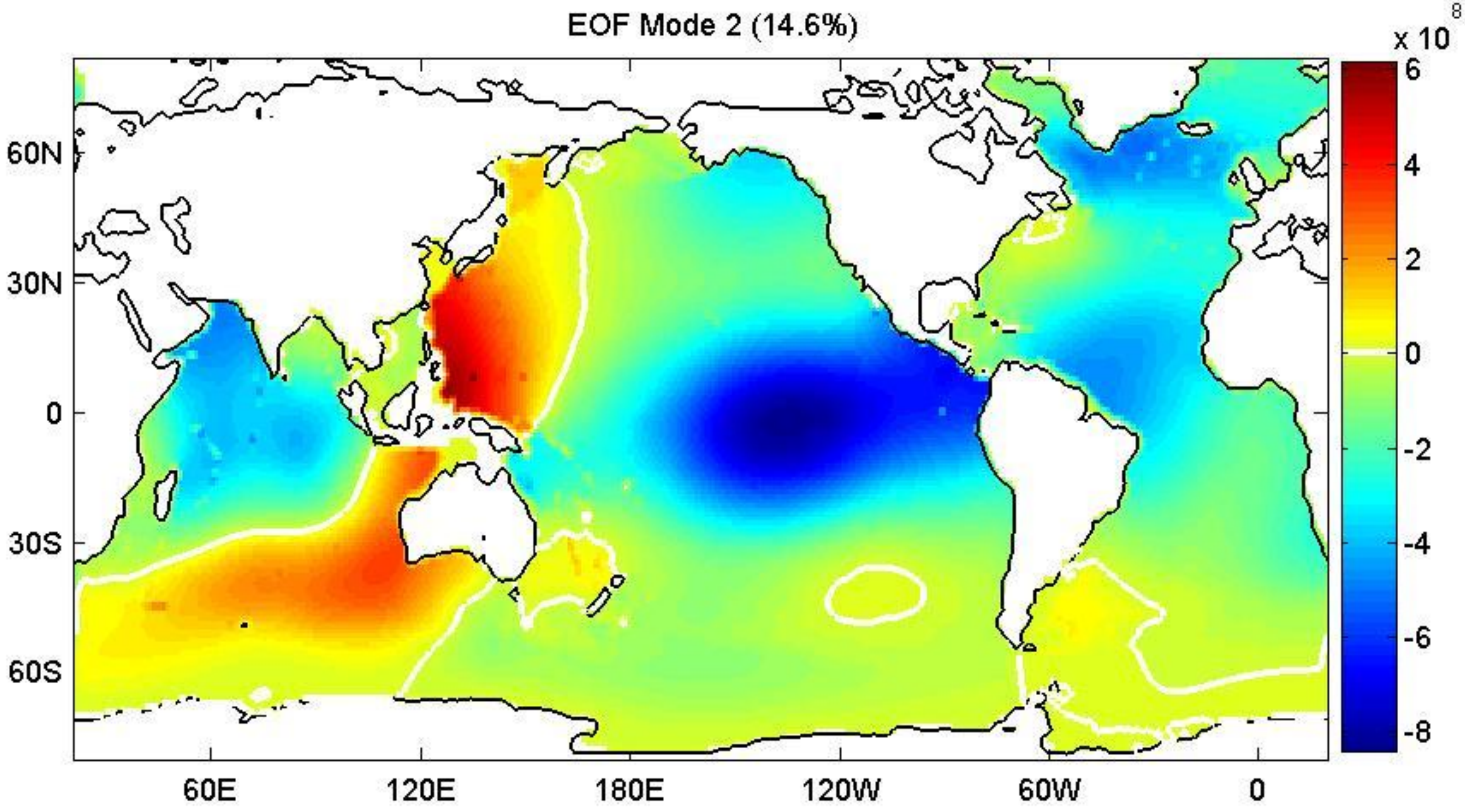

EOF-2 (in 10^8 J/m^2)

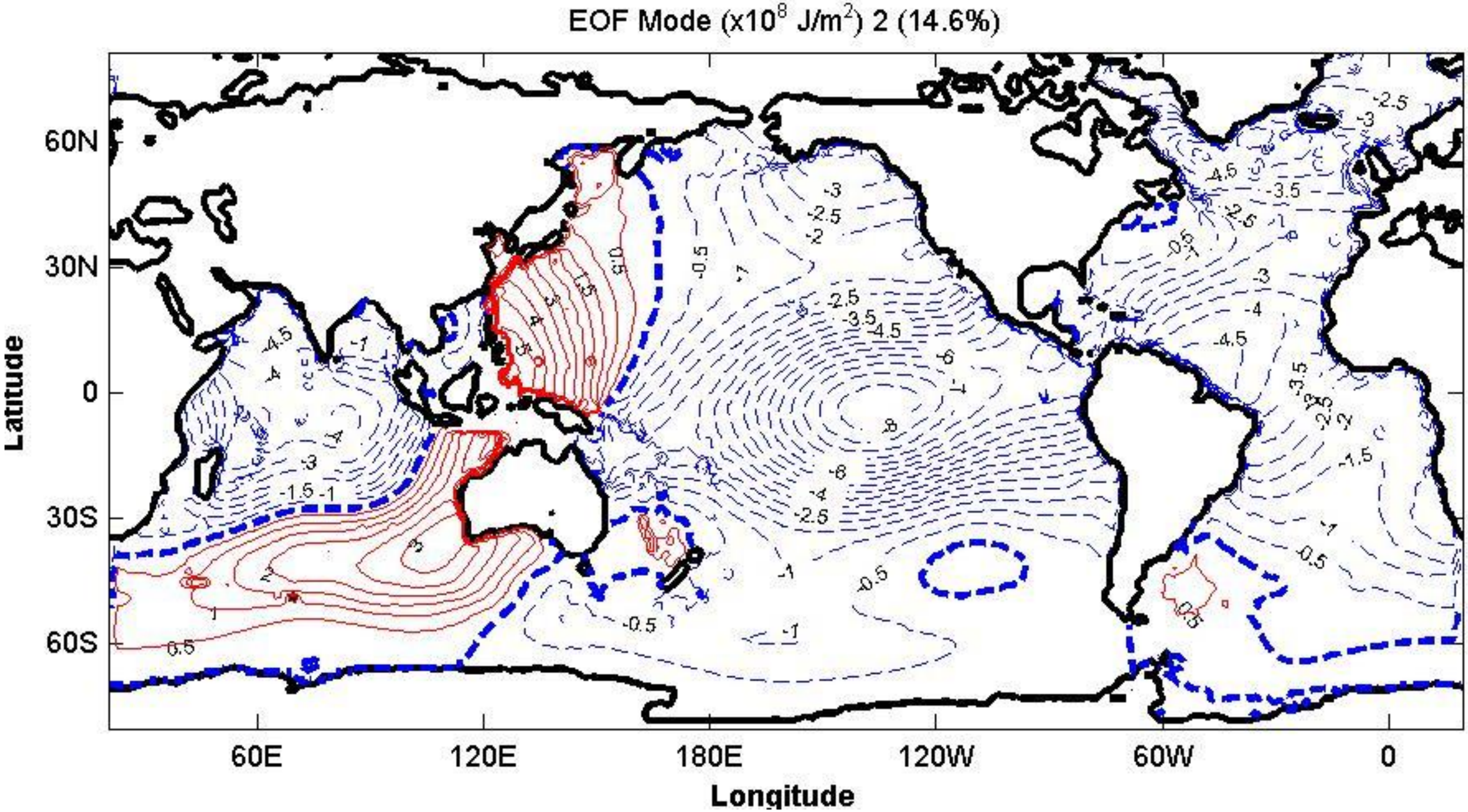

PC_2

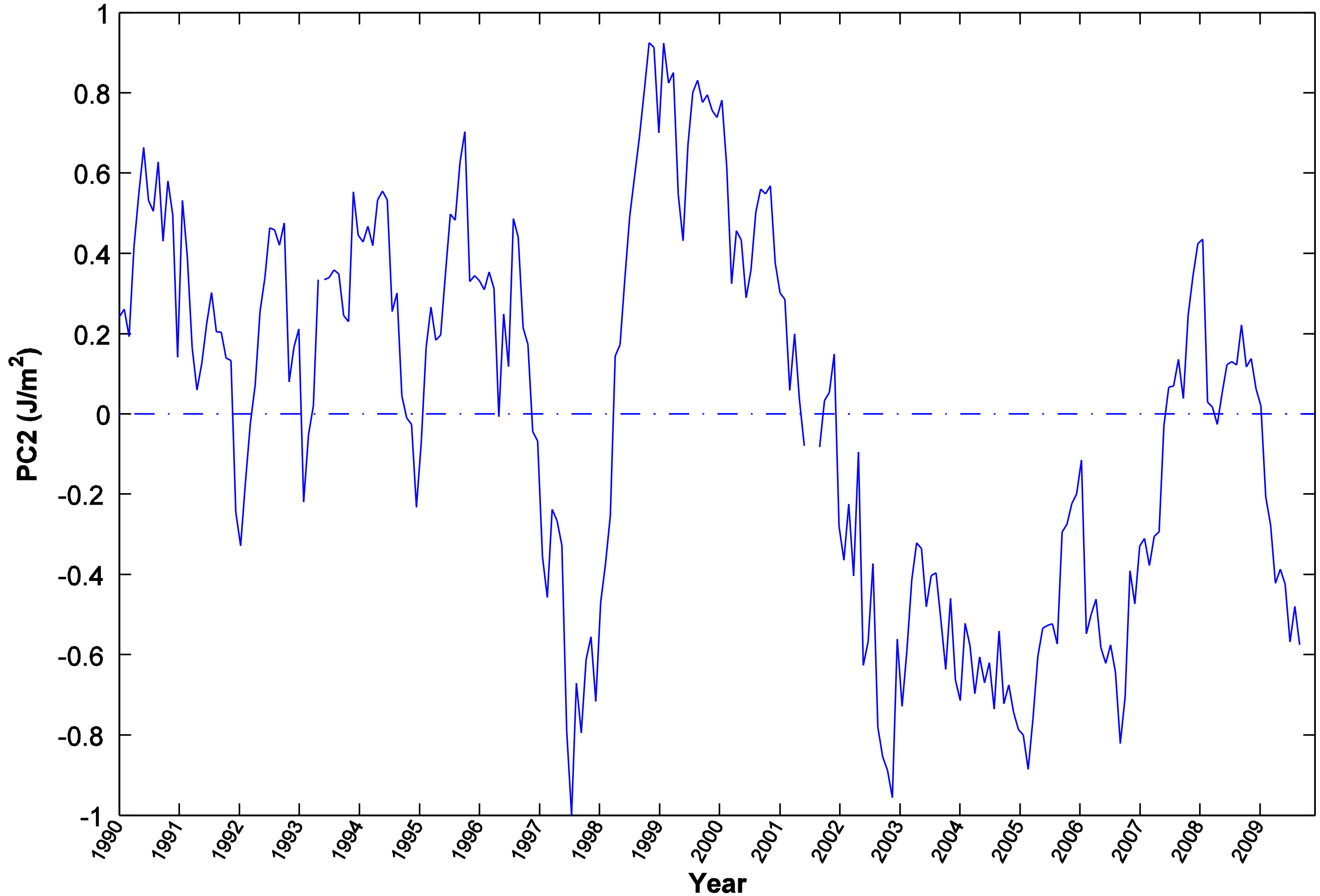

1
0.8
0.6
0.4
0.2
0
-0.2
-0.4
-0.6
-0.8
-1
PC2 (J/m2)
1990
1991
1992
1993
1994
1995
1996
1997
1998
1999
2000
2001
2002
2003
2004
2005
2006
2007
2008
2009
Year

Lag Correlation between PC_2 and SOI

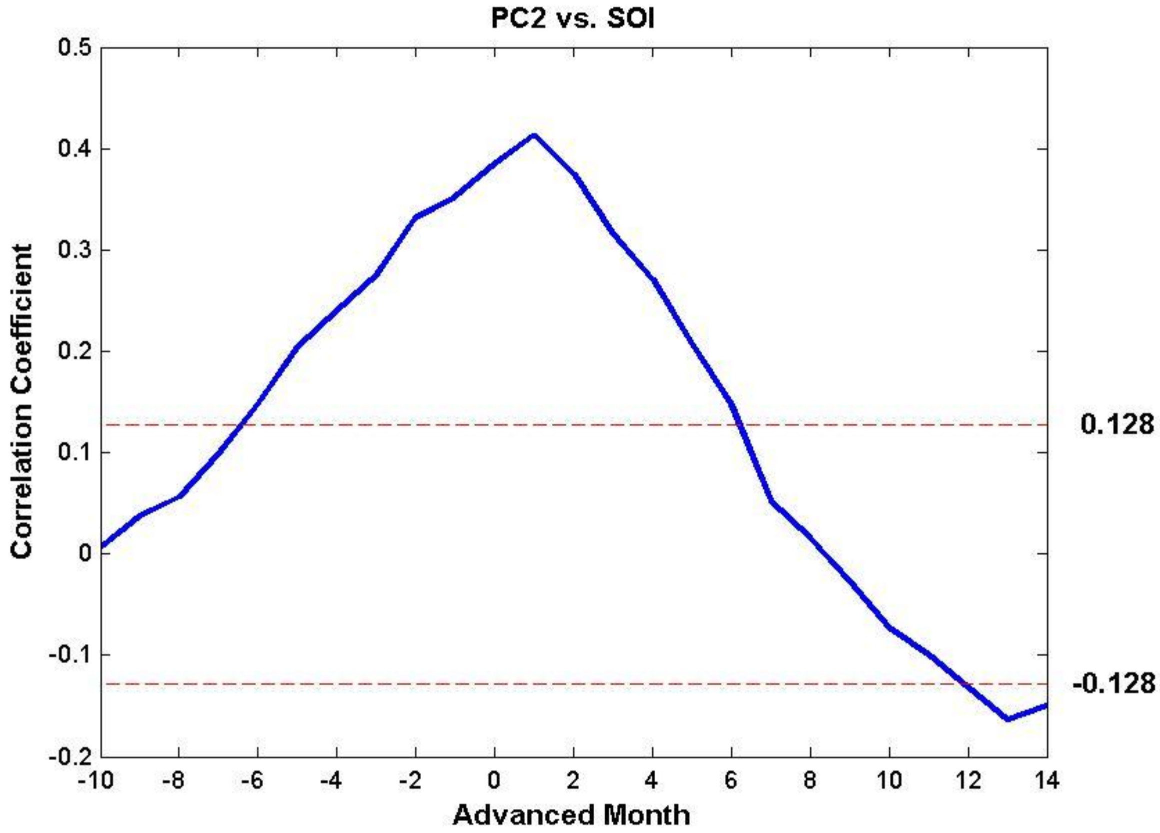

Positive Month → PC_2 advancing SOI

(4) Global Ocean Tripole

Canonical La Nina →
More and Stronger Hurricanes in Atlantic
(Pielke and Landsea, 1999 BAMS)

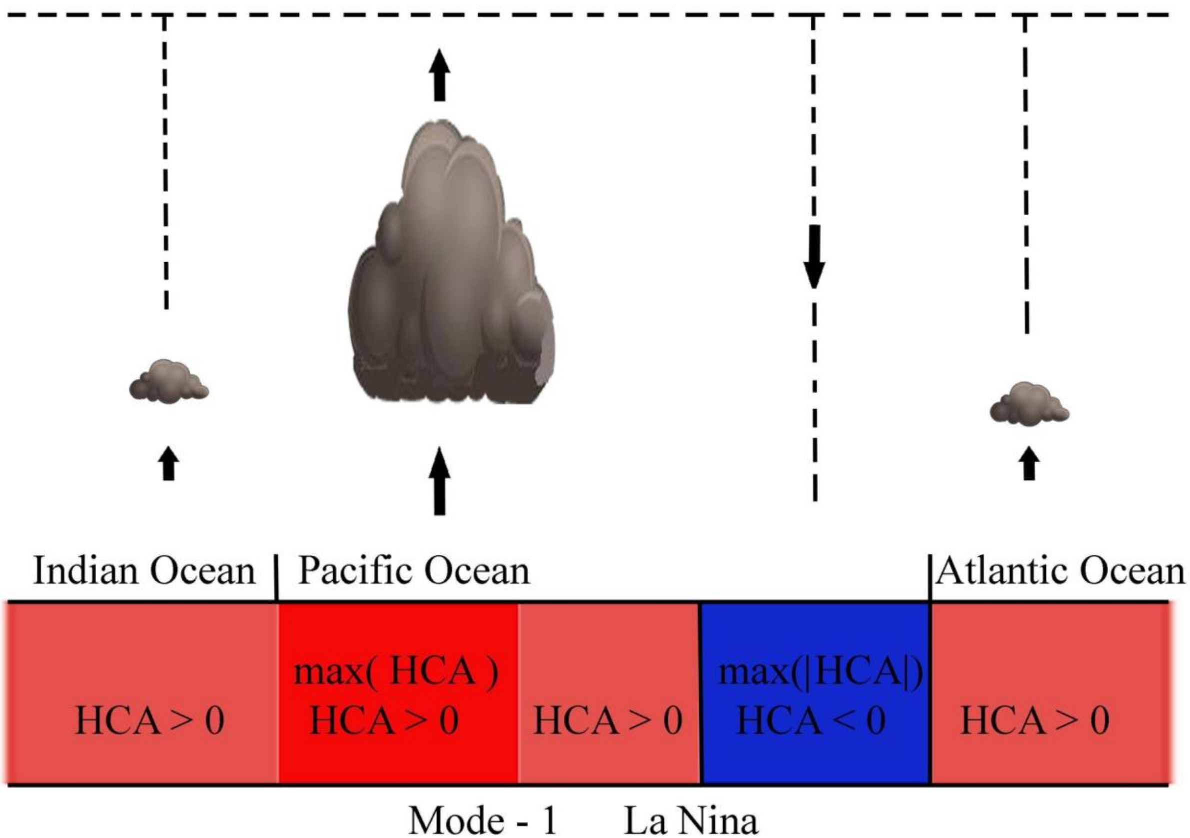

Canonical El Nino

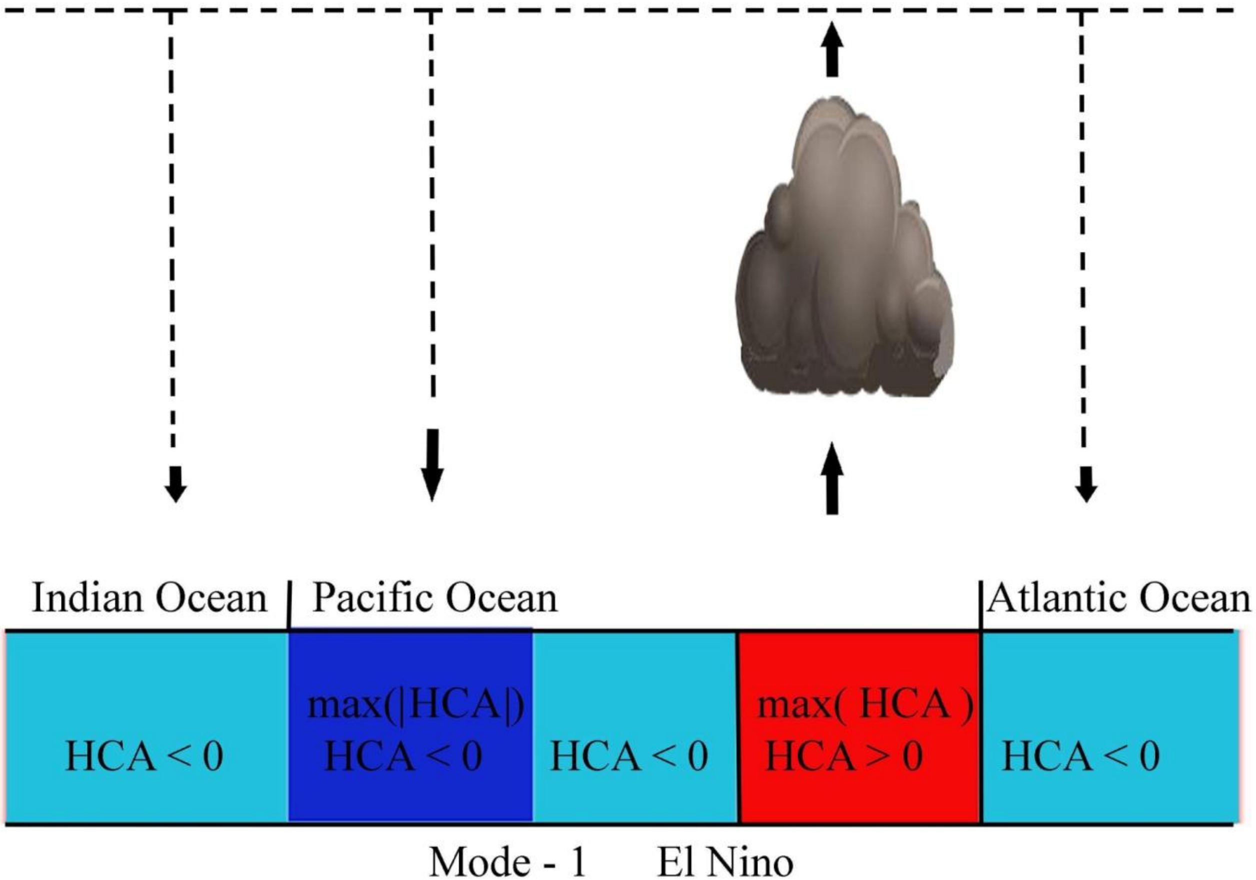

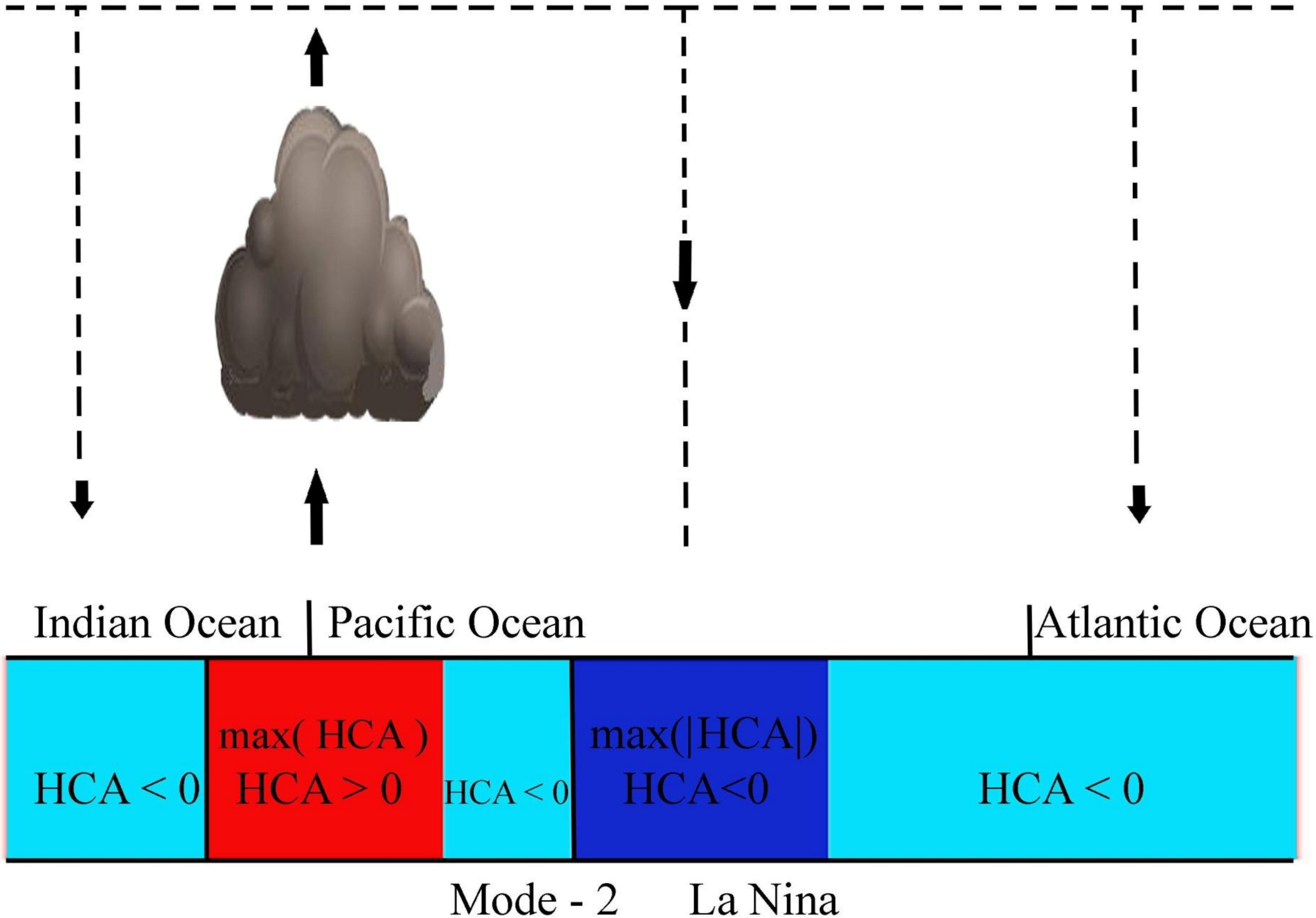
Indian Ocean
Pacific Ocean
Atlantic Ocean
HCA < 0
max(HCA)
HCA > 0
HCA < 0
max(|HCA|)
HCA<0
HCA < 0
Mode - 2
La Nina

El Nino Modoki

More and Stronger Hurricanes in Atlantic

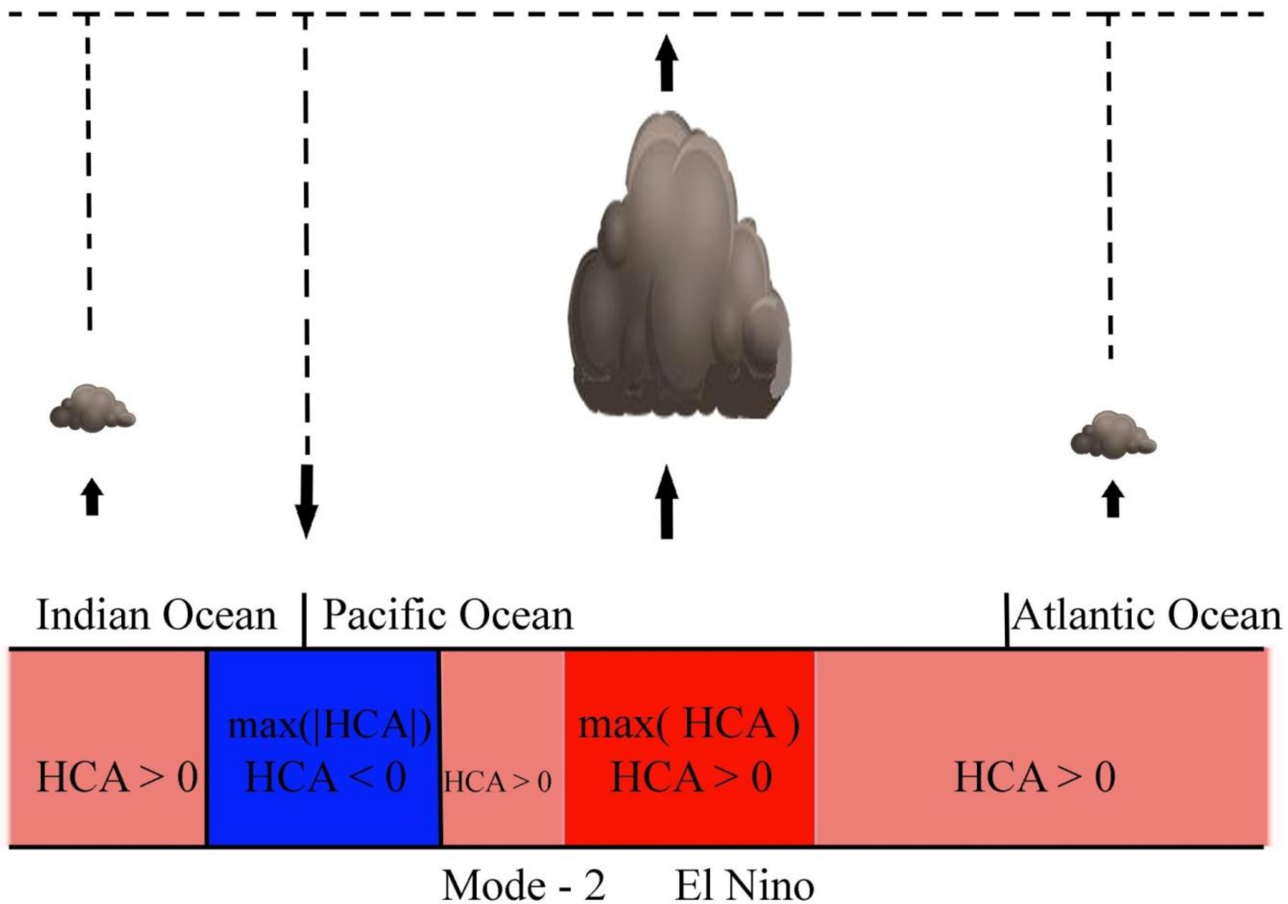

Trajectory in Phase Space (PC_1, PC_2)

- Blue Curve → La Nina

- Red Curve → Two Types of El Nino

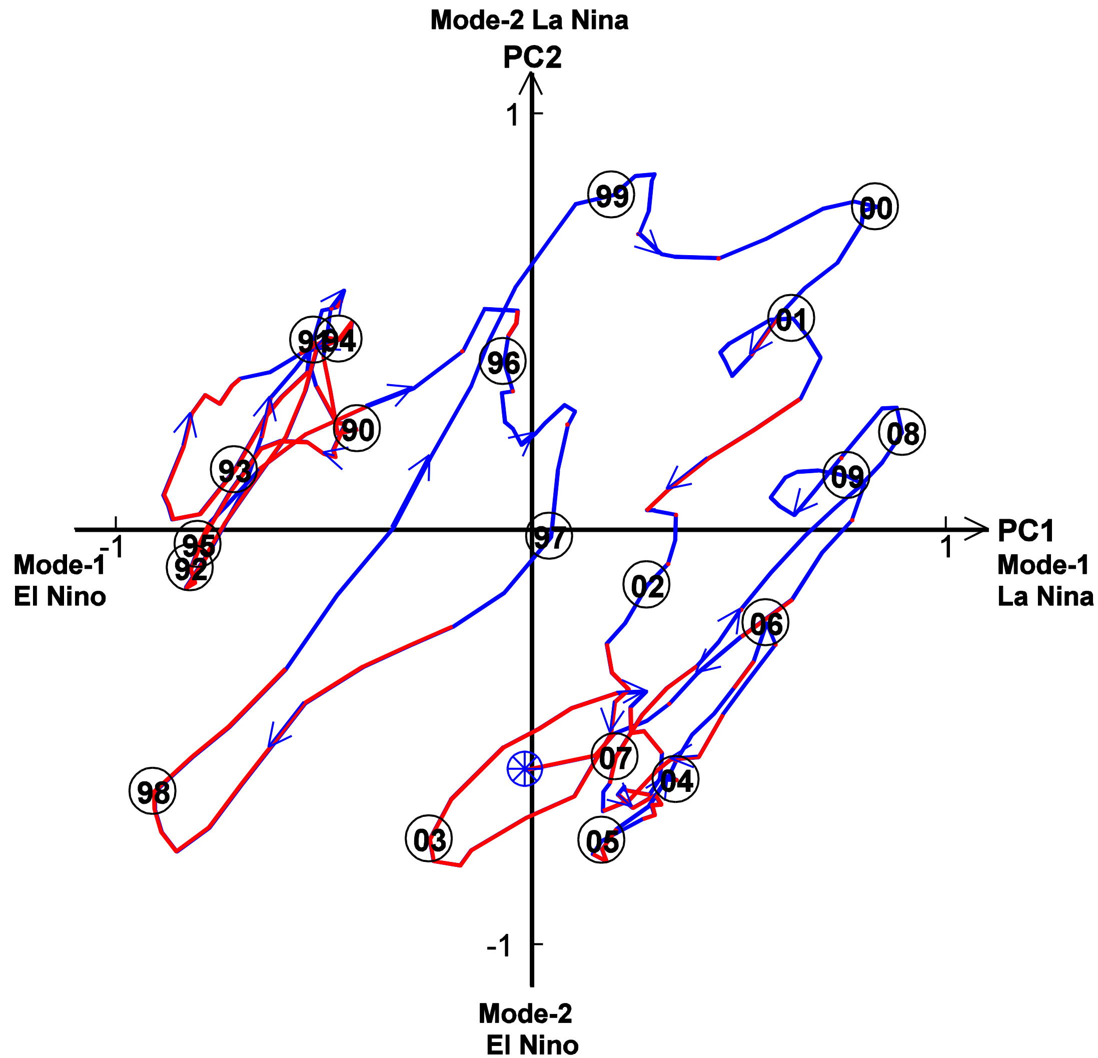

Conclusions

- (1) Upper ocean heat content contains the signal for climate change (interannual) → Global Ocean Tripole.

- (2) El Nino, El Nino Modoki, and Indian Ocean Dipole can be unified by Global Ocean Tripole.

Future Improvement

- Upper ocean heat content should not be calculated to a fixed depth such as 300 m in this study.
- Heat content in ocean mixed layer should be most important for the climate change.
- There is no simple, objective and effective method to determine mixed layer depth from profile data.
- My near future work is to develop such a method.